19th Australasian Fluid Mechanics Conference
Melbourne, Australia
8-11 December 2014

A New Model for Wake Effects Upon a Cantilevered Flexible Plate Undergoing Continuous Oscillation due to a High Reynolds-number Axial Flow

R.O.G. Evetts[1], R.M. Howell[1] and A.D. Lucey[1]

[1]Fluid Dynamics Research Group, Department of Mechanical Engineering,
Curtin University of Technology, GPO Box U1987,
Perth, Western Australia 6845, Australia

Abstract

We present two variations of a novel method that models the infinite-time response of the linearised motion of a cantilevered plate in ideal flow including the effect of the downstream wake. The inclusion of the wake effect in this eigenvalue problem is achieved by modelling the wake using a single vortex. To test the validity of the new models, we compare our results to those of a time-dependent numerical simulation that we have developed and which includes a distributed vorticity model of the wake. It is shown that the single-vortex models are capable of predicting the same trend in wake effect, found using the distributed vorticity model, stabilising the system at lower mass ratios and destabilising the system at higher mass ratios. It is also shown that varying the fluid density while maintaining a constant mass ratio and plate specific mass changes the critical velocity. Thus, a system which includes the wake cannot be characterised solely by the mass ratio and non-dimensional flow speed as is the case for the same system when the wake is omitted.

Introduction

A new model is developed of the linearised fluid-structure interaction (FSI) of a cantilevered plate of length L in a uniform axial flow of velocity U_∞ including the full wake generated by the oscillating plate, shown in figure 1. Inviscid flow is assumed, although viscous effects are implicitly incorporated through a Kutta condition; thus, the FSI model is relevant to the infinite limit of high Reynolds number flows that predominate in engineering applications. At these high Reynolds numbers, previous approaches have only been able to model this system via initial-value problem methods or using quasi-boundary-value problem methods that incorporate some form of time stepping, see [1-5, 8]. The present approach yields the full spectrum of possible system states after motions associated with system start-up have been damped out or convected away downstream.

The present modelling is based upon that of [4] that couches the governing equations in such a way that a companion-matrix is formed from which the system eigenvalues can be extracted giving the infinite-time solution of the system. Good agreement is found between this new method and the numerical-simulation results also presented in [4] once sufficient time has passed in the latter.

Good agreement continues to be found when the discretization of the wake is reduced, *i.e.* how often through a cycle of plate oscillation we choose to shed the change in bound vorticity. Coarsening the discretization leads to a wake model comprising a single, lumped wake vortex, at a downstream distance represented by the product of a full period of oscillation and the free-stream flow speed. Startlingly, this very simple model continues to yield very useful quantitative approximations of the effect of the wake on the stability of the flexible plate.

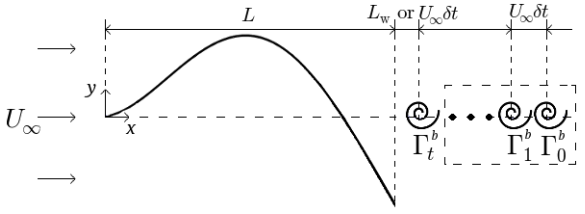

Figure 1: The fluid-structure system being examined. Those vortices in the dashed box apply only to the full numerical simulation.

The present model is used to show that, as predicted by several previous studies, the wake is stabilizing for single-mode flutter instability whereas it is destabilizing for the modal-coalescence type instability associated with plates of high mass ratio (plate length for given mass per unit area and fluid density). However, a new effect is found: if the thin plate condition is approached whilst keeping the mass ratio constant, the overall phenomenology of the wake effect changes. Thus, whilst maintaining the plate material properties constant we find that reducing the plate length while commensurately increasing the fluid density the aforementioned effects of the wake on single-mode flutter and modal-coalescence no longer hold. Overall, these results demonstrate that when wake effects are included, this canonical FSI system can no longer be fully characterised by just the non-dimensional mass ratio and flow speed.

Theoretical Modelling

The computational modelling continues from that developed in [4], in which the set-up of the initial- and boundary-value problems are described in detail. A one-dimensional Euler-Bernoulli beam is used to model the cantilever that in discretised matrix-form is equated as

$$\rho h[\mathbf{I}]\{\ddot{\eta}\} + B[\mathbf{D_4}]\{\eta\} \;=\; -\{\delta p\}. \qquad (1)$$

η is the vertical deflection of any of the N mass points along the beam, $[\mathbf{I}]$ is an identity matrix and $[\mathbf{D_4}]$ is a 4th-order spatial differentiation matrix. ρ, h, and B are respectively the density, thickness and flexural rigidity of the beam and δp is the pressure due to the fluid acting on the beam. A boundary-element method that utilises first-order vortices is used to model the fluid velocity: vortices are employed as the cantilever is a lifting surface. The surface is discretised into N panels of length $\delta x = L/N$ and the bound vortex-strengths γ are distributed over each individual panel. The solution for the bound vorticity comes from enforcing a boundary condition of zero normal-flow across the plate and is formulated as

$$\{\gamma\} \;=\; [\mathbf{I}^N]^{-1}\left\{U_\infty \theta + \dot{\eta}^{\mathrm{av}} - u^{N_b}\right\}. \qquad (2)$$

$[\mathbf{I}^N]$ contains the normal influence-coefficients and the additional boundary conditions of a Kutta condition at the trailing edge of the plate and continuity of vorticity strength between panels. ρ_f is the fluid density, θ is the linearised panel slope and $\dot{\eta}^{\mathrm{av}}$ is the average velocity between beam mass points. u^{N_b} is the normal velocity induced by the wake vortices at the mass points and is calculated as $\left[\mathbf{I}^{N_b}\right]\{\Gamma^b\}$, where Γ^b are the wake vortex strengths at discrete points in the wake trailing downstream of the cantilever and $\left[\mathbf{I}^{N_b}\right]$ is a matrix containing the

normal influence coefficients of the wake on the plate. The unsteady Bernoulli equation is used to quantify the pressure of the fluid and wake, the matrix form of which is

$$-\{\delta p\} \;=\; 2\rho_{\mathrm{f}} U_\infty v^{T'} + \rho_{\mathrm{f}} \frac{\partial \phi}{\partial t}, \qquad (3)$$

where the tangential-perturbation velocity $v^{T'}$ and the unsteady velocity-potential $\partial\phi/\partial t$ are equal to $\left[\mathbf{I}^{T}\right]\{\gamma\}$ and $\left[\mathbf{I}^{\phi}\right]\{\dot{\gamma}\}$ respectively. The wake is linearised and so the wake vortices only move horizontally and hence they induce zero tangential-velocity at the mass points, for example see [4] and [8]. Substituting equation (2) into equation (3) and expanding gives,

$$\begin{aligned} -\{\delta p\} \;&=\; 2\rho_{\mathrm{f}} U_\infty^2 [\mathbf{A}^-]\{\eta\} \;+\; \rho_{\mathrm{f}} U_\infty [\mathbf{A}^+]\{\dot{\eta}\} \\ &+\; \rho_{\mathrm{f}} U_\infty [\mathbf{B}^-]\{\dot{\eta}\} \;+\; \rho_{\mathrm{f}} [\mathbf{B}]\{\ddot{\eta}\} \;-\; \{\delta p\}^b, \quad (4) \end{aligned}$$

where $[\mathbf{A}]$ and $[\mathbf{B}]$ are rearranged forms of influence coefficient matrices. Depending on how the wake is modelled determines the formulation of $\{\delta p\}^b$: the other pressure terms are independent of the wake model. Substituting equation (4) into equation (1) and rearranging for $\{\ddot{\eta}\}$ yields

$$\{\ddot{\eta}\} \;=\; [\mathbf{E}]\{\dot{\eta}\} + [\mathbf{F}]\{\eta\} - [\mathbf{G}]\{u^{N_b}\} - [\mathbf{H}]\{\dot{u}^{N_b}\}. \qquad (5)$$

Below we detail two methods of solution of equation (5) and the three different wake models that we employ that lead to different forms of the matrices $[\mathbf{E}]$, $[\mathbf{F}]$, $[\mathbf{G}]$ and $[\mathbf{H}]$.

Full Numerical Simulation

This model is fully described in [4]: the vertical displacement of the mass points is calculated iteratively at a series of time steps after an initial deflection of the plate is applied to begin the simulation. A wake vortex is shed every time step and has a strength equal to the difference between the total vorticity at time $t = 0$, the vorticity bound within the plate at time t, and the sum vorticity contained within the wake (excluding the vortex forming at time t). At each time step this enforces the Kelvin condition, that there is no change in circulation within a closed system in time. Vortices enter the wake a distance $U_\infty \delta t$ from the trailing edge and maintain this distance between other wake vortices - see figure 1 - where δt is the time step size. A *cut-off length* of the wake is set as $2L$ and wake vortices that convect pass this point are removed and have their strengths summed into a far-wake strength variable. For this method equation (2) remains unchanged and so following the derivation of equation (4) above $\{\delta p\}^b$ for the full numerical simulation is

$$-\{\delta p\}^b_{\mathrm{ns}} \;=\; -2\rho_{\mathrm{f}} U_\infty [\mathbf{A}]\{u^{N_b}\} - \rho_{\mathrm{f}} [\mathbf{B}]\{\dot{u}^{N_b}\}. \qquad (6)$$

The forms of the matrices in equation (5) for this method are fully detailed in [4].

Eigenanalysis

Here a boundary-value type model is employed to calculate the infinite-time solution of the fluid-structure problem using a state-space method. Equating the state-space variables as $w_1(t) = \eta(t)$, $w_2(t) = \dot{\eta}(t) = \dot{w}_1(t)$ and therefore $\dot{w}_2(t) = \ddot{\eta}(t)$ enables the reduction of the order of the problem from second- to first-order and dictates the formulation of the $(2N \times 2N)$ companion-form matrix. Once the companion form has been assembled the $2N$ eigenvalues are extracted: these have both a real and imaginary component that quantify the system stability and oscillation frequency respectively. To enable formulation of an infinite-time solution that includes wake effects, the wake is approximated as a single vortex: this allows u^{Nb} in equation (2) to be described entirely in terms of η and $\dot{\eta}$. This enables simplification of equation (5) as the matrices $[\mathbf{G}]$ and $[\mathbf{H}]$ are no longer required. The strength of the wake vortex based on two different interpretations of the Kelvin condition are

$$\Gamma^b \;=\; \sum \dot{\gamma} \delta x T \quad \text{and} \quad \Gamma^b \;=\; -\sum \gamma \delta x. \qquad (7a,\, b)$$

Model 1: Equation (7a) enforces that the wake vortex must have a strength equal to the change in bound vorticity during an oscillation of the cantilever. The wake vortex is placed a distance L_w downstream of the trailing edge where $L_w = U_\infty T$, T being the period of oscillation. Equation (7a) is applied in equation (2); inserting the latter into equation (3) the pressure contribution from the wake is

$$-\{\delta p\}^b_1 \;=\; -\rho_{\mathrm{f}} L_w (2U_\infty [\mathbf{P}]\{\dot{\eta}\} + 2[\mathbf{Q}]\{\ddot{\eta}\} + [\mathbf{R}]\{\dddot{\eta}\}), \quad (8)$$

where matrices $[\mathbf{P}]$, $[\mathbf{Q}]$ and $[\mathbf{R}]$ are further rearranged influence coefficients. Inserting equation (8) into equation (4) and rearranging into the form of equation (5) yields

$$\begin{aligned} [\mathbf{E}]_1 \;&=\; [\mathbf{C}]_1^{-1} \left[\rho_{\mathrm{f}} U_\infty \left(\left[\mathbf{A}^+\right] + \left[\mathbf{B}^-\right] - 2L_w [\mathbf{P}] \right) \right], \quad (9) \\ [\mathbf{F}]_1 \;&=\; [\mathbf{C}]_1^{-1} \left[2\rho_{\mathrm{f}} U_\infty^2 \left[\mathbf{A}^-\right] - B[\bigtriangledown^4] \right], \quad (10) \\ [\mathbf{C}]_1 \;&=\; \left[\rho h [\mathbf{I}] - \rho_{\mathrm{f}} [\mathbf{B}] + 2\rho_{\mathrm{f}} L_w [\mathbf{Q}] + \rho_{\mathrm{f}} L_w [\mathbf{R}] \right]. \quad (11) \end{aligned}$$

An initial guess for L_w is made and several iterations of the system are required to finalise the location of the wake vortex. The temporal change in wake strength present in equation (7a) gives rise to a *jerk* term that is a third-order time derivative of η: to retain the $(2N \times 2N)$ shape of the state-space companion matrix we neglect this term - the validity of this omission is tested using the initial-value method in the results section below.

Model 2: Equation (7b), used in [2], states that the vorticity in the wake is equal and opposite to that in the cantilever at all times. Applying this equation in the same fashion as in Model 1 above, the pressure contribution from the wake in this case is

$$-\{\delta p\}^b_2 = -\rho_{\mathrm{f}} (2U_\infty^2 [\mathbf{P}]\{\eta\} + U_\infty [\mathbf{Q} + \mathbf{R}]\{\dot{\eta}\} + [\mathbf{S}]\{\ddot{\eta}\}), \quad (12)$$

where $[\mathbf{S}]$ is a further rearranged form of influence coefficient matrices. Inserting equation (12) into equation (4) and rearranging into the form of equation (5) yields

$$\begin{aligned} [\mathbf{E}]_2 \;&=\; [\mathbf{C}]_2^{-1} \left[\rho_{\mathrm{f}} U_\infty \left(\left[\mathbf{A}^+\right] + \left[\mathbf{B}^-\right] - [\mathbf{Q}] - [\mathbf{R}] \right) \right], \quad (13) \\ [\mathbf{F}]_2 \;&=\; [\mathbf{C}]_2^{-1} \left[2\rho_{\mathrm{f}} U_\infty^2 \left(\left[\mathbf{A}^-\right] - [\mathbf{P}] \right) - B[\bigtriangledown^4] \right], \quad (14) \\ [\mathbf{C}]_2 \;&=\; [\rho h [\mathbf{I}] - \rho_{\mathrm{f}} [\mathbf{B}] + \rho_{\mathrm{f}} [\mathbf{S}]]. \quad (15) \end{aligned}$$

The jerk term does not arise in this second model as there is no time differential of the lumped-vortex strength in equation (7b); therefore, L_w is also absent from equation (7b) as there is now no need to balance the additional time term - however, the wake vortex is still located at L_w from the trailing edge of the plate and it is still required to iterate for its final magnitude.

Results

The focus of the results is upon the critical (lowest) speed after which flutter of the flexible plate first occurs. Previous studies (e.g. [4]) have shown that the behaviour of the FSI system can be described by two control parameters, namely the non-dimensional flow speed $\bar{U} = U_\infty (\rho h)^{3/2} / (\rho_{\mathrm{f}} B^{1/2})$ and the fluid-to-plate mass ratio $\bar{L} = \rho_{\mathrm{f}} L / (\rho h)$ and thus we use these parameters herein. To validate our modelling we first compare our results to those in [4] that were comprehensively assessed against those of other computational and theoretical models in the literature. Thereafter we present results of various simplifications to the model for the purposes of generating our more versatile boundary-value models. Finally the effects of varying the density of the fluid and length of the cantilever while maintaining a constant mass ratio are presented. In what follows

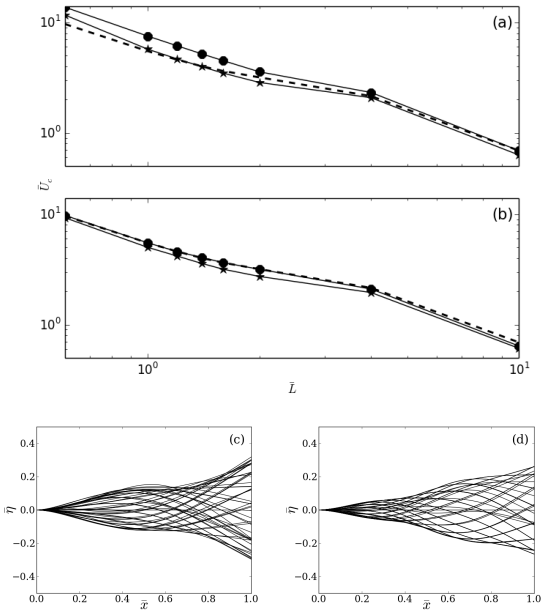

Figure 2: Results from the numerical simulation of the initial-value model for (a) fully discretised wake model, and (b) wake modelled by a single vortex. In each of these the no-wake, full (with jerk) and no-jerk results are shown by - - -, $\star$ and $\bullet$ respectively. (c) and (d) show the plate deflections over one oscillation for $\bar{L} = 1$ and 10 using the full numerical simulation model.

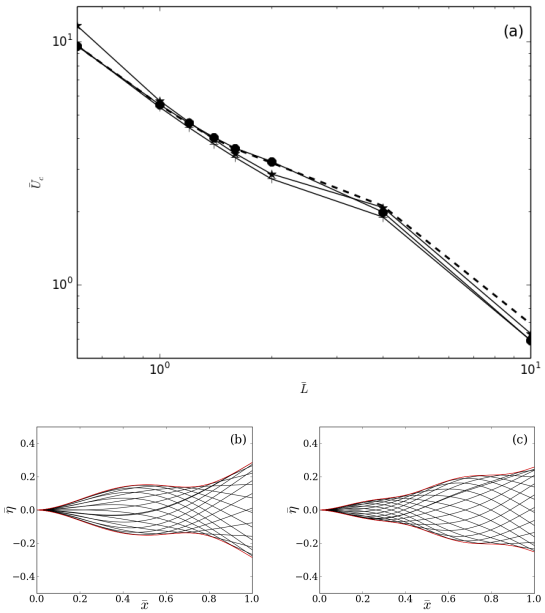

Figure 3: (a) A comparison of instability-onset flow speeds obtained from the two boundary-value models, $+$ using equation (7a) (with jerk omitted) and $\bullet$ using equation (7b), with the results of numerical simulations, $\star$ with a fully discretised wake and - - - with no wake. (b) and (c) show the plate deflections over one oscillation for $\bar{L} = 1$ and 10 using **model 1**.

$\bar{U}_c^*$ and $\bar{U}_c$ are the critical non-dimensional flow velocities at which instability occurs with and without a wake respectively. When plotting plate deflections the non-dimensional forms of distance along the plate and the plate deflection are $\bar{x}(= x/L)$ and $\bar{\eta}$; in the latter, values of η are normalised by the value of initial maximum-deflection for the initial-value problem or the overall maximum-deflection for the boundary-value problem.

Initial-value (Numerical Simulation) Results

Table 1 lists the critical flow speeds predicted by the current model without and with a wake, comparing the latter with the corresponding results in [4] along with percentage difference between the two. Very good agreement is seen and by comparing these critical speeds with those predicted in the absence of a wake, the effect of the wake on the FSI system is seen to be stabilising for plates with low $\bar{L}$ and destabilising for plates with high $\bar{L}$; an explanation for this is given in [4].

To examine the effect of the jerk on the system and to judge the appropriateness of its omission in the two boundary-value models, we assessed simpler versions of the initial value model. First, the fully discretised wake was replaced by a single vortex and, second, the jerk term was removed from both the fully discretised wake and single-vortex models. Figures 2 (a) and (b) show the variations of critical speed with mass ratio for these simplifications along with the results of the fully discretised wake (in (a) only) and the results in the complete absence of a the wake. Overall these results show that (i) when jerk is omitted, the model over-predicts the critical speed, and (ii) when a single-vortex is used to represent the wake, the critical speed is under-predicted. However, it is evident that the single-vortex approximation, either with or without jerk, yields results that are very close to those when a full discretisation of the wake is applied and certainly good enough for engineering predictions and the basis to develop a more versatile boundary-value solution for the system incorporating a wake.

$\bar{\mathbf{L}}$	$\bar{\mathbf{U}}_\mathbf{c}$	$\bar{\mathbf{U}}_\mathbf{c}^*$[4]	$\bar{\mathbf{U}}_\mathbf{c}^*$	**% Difference**
0.6	9.65	11.47	11.65	1.57
1.0	5.50	5.95	5.73	3.70
1.2	4.60	4.73	4.68	1.06
1.4	4.01	3.95	3.97	0.51
1.6	3.63	3.44	3.47	0.87

Table 1: Dependence of critical speed on mass ratio (non-dimensional plate length) and comparison between current results and those of [4].

Figures 2 (c) and (d) show the instability-mode deformations at low and high mass ratios for which the effect of the wake is respectively stabilising and destabilising, a difference that also occurs for the models that omit the jerk term. At the lower mass ratio flutter is dominated by second-mode content while at the higher mass ratio the flutter displays both second- and third-mode contributions; the former is described as a single-mode flutter and the latter a modal-coalescence flutter. These findings agree with the results of [4] and [8]. It is also noted that as the mass ratio increases, yielding critical modes of higher order, the effect of the wake on the stability of the flexible plate becomes negligible.

Boundary-value Results

The predictions of instability-onset flow speed for the two boundary-value models developed in this paper are shown in figure 3 (a) and compared to the model without a wake. Also included in this figure is the result from numerical simulations using a fully discretised wake and which also appeared as the solid line figure 2 (a); this is the most complete model against which the more economical boundary-value results are assessed. It is seen that the first boundary-value model, developed using equation (7a), yields results that compare well against this benchmark for $\bar{L} \succeq 1$ while the second model (that uses equation (7b)) gives results that are very similar to those when the wake is absent. Figures 3 (b) and (c) show the mode shapes predicted by the first boundary-value model and correspond to figures 2 (c) and (d) obtained using full numerical simulation; again very good agreement is seen. Thus, the first boundary-value model provides an accurate but simpler alternative for the prediction of the long-time response of the system when the mass ratio is approximately greater than unity.

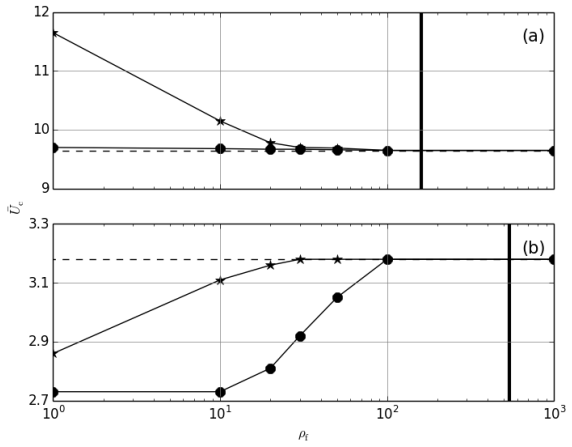

Figure 4: Variation of critical velocities with fluid density for constant $\bar{L}$ values. Each line is the critical velocity given by: numerical simulation with $\star$ for a fully discretised wake and - - - for no wake, and $\bullet$ the first boundary-value model with a wake (noting that with the wake effects suppressed, this model gives the same results as the numerical simulation without a wake). The limit of the thin plate assumption where $L/h \geq 10$ is shown by the thick vertical line. (a) $\bar{L} = 0.6$, (b) $\bar{L} = 2.0$.

Fluid Density Variations

Although presented in non-dimensional form, all of the preceding results were obtained using air $\rho_f = 1.2$ kg/m^3 as the fluid. The wake models developed in this paper have also been used with fluids of much higher densities to assess whether the non-dimensionalisation of the system is complete. Figure 4 shows the variation of the non-dimensional instability-onset flow speed for two mass ratios, $\bar{L} = 0.6$ and 2.0, in which the fluid density is varied but holding constant the value of $\rho_f L$ and maintaining the plate material properties at $\rho h = 1.355$ kg/m^2. The figure includes the numerical-simulation results from the fully discretised wake and the case where the wake is omitted, along with the predictions of the first boundary-value model that was found to give a more accurate representation of wake effects in the foregoing sub-section. There is no variation of critical speed when the wake is absent and this demonstrates that $\bar{L}$ and $\bar{U}$ fully describe the system. However, when the wake is included, the critical speed does depend upon the fluid density and the commensurate change in plate length; as density is increased the critical speed asymptotes to that when the wake is absent. In figure 4 (a) the dependence upon fluid density (and plate length) is only found for the numerical simulation results because the boundary-value model was seen to be inappropriate at $\bar{L} \preceq 1$ while in figure 4 (b) both the full and approximate methods give variations to $\bar{U}_c$ that are in reasonable agreement. In total these results show that the wake effects - stabilising for low $\bar{L}$ and mildly destabilising for high $\bar{L}$ - only apply for fluids with low density as compared with that of the structure.

To explain these new findings, we report that the position of the single wake vortex in the boundary-value problem is found to move further downstream for higher-density fluids to a distance of between 2 and 2.5 flexible-plate lengths, whereas in lower-density fluids the vortex is between 0.05 and 0.3 flexible-plate lengths downstream of its trailing edge. This explains why the critical flow speeds converge to no-wake results as the fluid density is increased; the wake vorticity is too distant for it to have an appreciable effect. For a given mass ratio, the distancing of wake-vorticity effect occurs because an increase in fluid density requires a shortening of the plate length. This latter requirement yields an increase to the oscillatory frequency of the flexible plate as it supersedes the effect of increased fluid inertia due to the higher density of the fluid used. The higher frequency then reduces the effective interaction of the wake and the motion of the flexible plate. Finally, the present results show that when the wake is modelled, the non-dimensionalised FSI system is no longer completely characterised by $\bar{U}$ and $\bar{L}$ because the fluid-to-solid density ratio ρ_f/ρ also becomes a control parameter.

Conclusions

In this paper a number of theoretical and computational models have been developed to investigate the effect of the wake on the stability of a cantilevered flexible plate in an ideal flow. Numerical simulations when a fully discretised wake is modelled show that the wake is stabilising(destabilising) for low(high) mass ratios as shown in [4]. The effect of the jerk (rate of change of acceleration) term is examined and its omission is shown to yield more stable predictions than those of the full system. Numerical simulations using just a single vortex to represent the wake are shown to yield predictions of instability onset that are in reasonable agreement with those of the faithfully represented distributed wake-vorticity model.

New models are developed that use the state-space method developed in [4] and [6] to solve the boundary-value problem when wake effects are incorporated. These new models show that it is possible to qualitatively capture the effect of a wake on a cantilevered plate using only a single wake vortex. In particular it is shown that a wake-shedding model based upon the Kelvin condition yields values of critical speed that are in very good agreement with full numerical simulations (after sufficient time has passed for transients to be convected away) when $\bar{L} \succeq 1$ for a much lower computational cost.

Finally a new result is found concerning the non-dimensional characterisation of the FSI system. In the absence of a wake, only two non-dimensional control parameters, the flow speed $\bar{U}$ and the mass ratio $\bar{L}$, fully describe the system behaviour, but when wake effects are included the fluid-to-solid density ratio must additionally be accounted for. The present results show that, for any fixed mass ratio, when the fluid-to-solid density ratio is low the wake effects on stability described in the opening paragraph are found to hold. However, as the density ratio is increased these wake effects decrease and for fluids with high density the wake has a negligible effect.

References

[1] Argentina, M. & Mahadevan, L., Fluid-flow-induced flutter of a flag, in *P. Natl. Acad. Sci. USA*, **102** (6), 2005, 1829–1834.

[2] Giesing, J.P., Nonlinear Interaction of Two Lifting Bodies in Arbitrary Unsteady Motion, *J. Fluids Eng.*, **90**, 1968, 387–394.

[3] Hall, K. C., Eigenanalysis of unsteady flows about airfoils, cascades, and wings, *AIAA J.*, **32** (12), 1994, 2426–2432.

[4] Howell, R.M., Lucey, A.D., Carpenter, P.W. and Pitman, M.W., Interaction between a cantilevered-free flexible plate and ideal flow, *J. Fluid Struc.*, **25**, 2009, 544–566.

[5] Michelin, S., Llewllyn Smith, S. G. & Glover, B. J., Vortex shedding model of a flapping flag, *J. Fluid Mech.*, **617**, 2008, 1–10.

[6] Pitman, M.W. and Lucey, A.D., On the direct determination of the eigenmodes of finite flow-structure systems, in *Proc. R. Soc. A*, **465**, 2009, 257–281.

[7] Tang, D. & Dowell, E. H., Limit cycle oscillations of two-dimensional panels in low subsonic flow, *Int. J. Nonlinear Mech.* **37**, 2002, 1199–1209.

[8] Tang, L. and Païdoussis, M.P., The influence of the wake on the stability of cantilevered flexible plates in axial flow, *J. Sound Vib.*, **310**, 2008, 512–526.